Magnetic Field-Induced Strain and Magnetoelectric Effects in Sandwich Composite of Ferromagnetic Shape Memory Ni-Mn-Ga Crystal and Piezoelectric PVDF Polymer

Min Zeng, Siu Wing Or, *Senior Member, IEEE*, and Helen Lai Wa Chan, *Senior Member, IEEE*

Abstract—A sandwich composite consisting of one layer of ferromagnetic shape memory Ni-Mn-Ga crystal plate bonded between two layers of piezoelectric PVDF polymer film was fabricated, and its magnetic field-induced strain (MFIS) and magnetoelectric (ME) effects were investigated, together with a monolithic Ni-Mn-Ga crystal, as functions of magnetic fields and mechanical load. The load-free dc- and ac-MFISs were 0.35 and 0.05% in the composite, and 5.6 and 0.3% in the monolithic crystal, respectively. The relatively smaller load-free MFISs in the composite than the monolithic crystal resulted from the clamping of martensitic twin-boundary motion in the Ni-Mn-Ga plate by the PVDF films. The largest ME coefficient (α_E) was 0.58 V/cm·Oe at a magnetic bias field (H_{Bias}) of 8.35 kOe under load-free condition. The mechanism of the ME effect originated from the mechanically mediated MFIS effect in the Ni-Mn-Ga plate and piezoelectric effect in the PVDF films. The measured α_E–H_{Bias} responses under different loads showed good agreement with the model prediction.

I. Introduction

FERROMAGNETIC shape memory (FSM) alloys have attracted great attention in recent years because of their ability to produce giant magnetic field-induced strains (MFISs) in the martensitic phase [1]–[8], which are one order of magnitude higher than the magnetostrictive strains of magnetostrictive alloys such as Terfenol-D [9]–[12]. The mechanism of giant MFISs in the FSM alloys is a reorientation of martensitic twin variants under an applied magnetic field as a result of magnetocrystalline anisotropy [1]–[3]. It is very different from the magnetostrictive alloys that generate strains through magnetic domain rotation [9]–[12]. Among the available FSM alloys, Ni-Mn-Ga crystals are regarded as one of the most promising candidates because their dc-MFISs are as large as 6 and 10%, respectively, in the 5M tetragonal and 7M

orthorhombic martensitic phases in load-free condition at room temperature [3], [4].

The magnetoelectric (ME) effect, which is an electric polarization response in a material to an applied magnetic field [13], has also received considerable interest because of its great potential for realizing power-free magnetic field sensors, electric current sensors, magnetoelectric transducers, current-to-voltage converters, etc. [14]. In fact, many ME materials have been developed in the past decade, including single-phase materials [15]–[17], multiphase bulk composites [18]–[21], and multiphase laminated composites [22]–[27]. Today, it is generally known that laminated composites of magnetostrictive (e.g., Terfenol-D alloy, ferrites, etc.) and piezoelectric (e.g., PZT ceramics, PMN–PT crystals, etc.) phases possess much higher ME effect than single-phase materials and bulk composites because of the mechanically mediated magnetostrictive effect in the magnetostrictive phase and the piezoelectric effect in the piezoelectric phase [14]–[26]. This suggests that the magnetostrictive and piezoelectric phases in the laminated composites function as a magnetomechanical actuator and a mechanoelectric sensor, respectively.

Because Ni-Mn-Ga crystals exhibit an interestingly large MFIS effect, it is expected that their laminated composites can enable a correspondingly large ME effect with a distinct physical mechanism compared with those comprising magnetostrictive phase. In this paper, we report experimentally and theoretically the large ME effect in a PVDF/Ni-Mn-Ga/PVDF sandwich composite caused by the mechanically mediated MFIS effect in the Ni-Mn-Ga crystal phase and piezoelectric effect in the PVDF polymer phase. On the other hand, because this sandwich composite is essentially an FSM composite (with both phases active), we also report its combined dc- and ac-MFIS effects, in conjunction with a monolithic Ni-Mn-Ga crystal, in terms of reorientation and configuration of martensitic twin variants under different applied magnetic fields and mechanical loads.

M. Zeng and S. W. Or are with the Department of Electrical Engineering, The Hong Kong Polytechnic University, Hung Hom, Kowloon, Hong Kong (e-mail: eeswor@polyu.edu.hk).

M. Zeng and H. L. W. Chan are with the Department of Applied Physics, The Hong Kong Polytechnic University, Hung Hom, Kowloon, Hong Kong.

II. Experimental Details

Fig. 1(a) shows the schematic diagram of the proposed PVDF/Ni-Mn-Ga/PVDF sandwich composite. In fabrica-
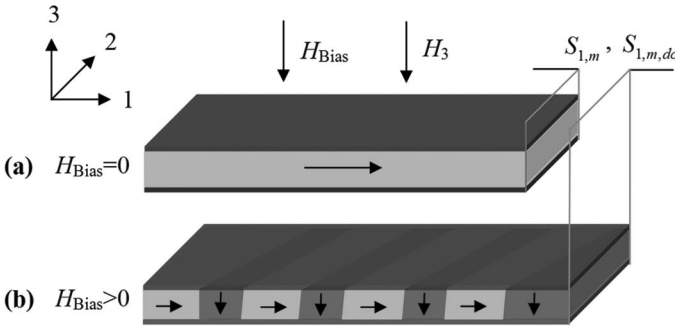
Fig. 1. Configuration and working principle of the PVDF/Ni-Mn-Ga/PVDF sandwich composite in the (a) absence and (b) presence of a dc magnetic bias field (H_{Bias}).

tion, the sandwich composite was formed by laminating one layer of FSM Ni-Mn-Ga crystal plate between two layers of piezoelectric PVDF polymer film. The Ni-Mn-Ga plate, with a chemical composition $Ni_{50}Mn_{29}Ga_{21}$, dimensions 19 mm (length) × 5 mm (width) × 3 mm (thickness), the two major surfaces parallel to the {011} planes, and a load-free dc-MFIS of 5.6% in the tetragonal martensitic phase at room temperature, was supplied by AdaptaMat Ltd. (Helsinki, Finland). The transformation temperatures were determined to be austenite start (A_s) = 38°C, austenite finish (A_f) = 41°C, martensite start (M_s) = 35°C, and martensite finish (M_f) = 33°C using a differential scanning calorimeter (DSC7, Perkin Elmer, Waltham, MA). The martensitic structure was found to be nearly tetragonal with the lattice parameters $a = b$ = 0.594 nm and c = 0.560 nm by an X-ray diffractometer (D8 Advance, Bruker AXS GmbH, Karlsruhe, Germany), giving the theoretical maximum lattice strain (ε_0 = 1 − c/a) of 5.7%. The easy (c) and hard (a and b) axes of magnetization were along the [001] and [100] / [010] directions, respectively, whereas the magnetocrystalline anisotropic constant (K_μ) was 176 kJ/m³, as evaluated from the magnetization-magnetic field (M–H) curve using a vibrating sample magnetometer (7600, Lakeshore, Westerville, OH). The PVDF films, having the same cross-sectional area as the Ni-Mn-Ga plate, a different thickness of 0.11 mm, an electric polarization along the thickness direction, and full-fired silver electrodes on the two major surfaces perpendicular to the thickness direction, were acquired from Measurement Specialties Inc. (Hampton, VA). To fabricate a PVDF/Ni-Mn-Ga/PVDF sandwich composite exhibiting the maximally allowable MFIS and ME effects, the length of the Ni-Mn-Ga plate was maximally shortened to preset an initial nearly single-variant state in the plate by applying a dc magnetic field of 1 T along its length direction. By keeping the field unchanged, two layers of PVDF film were bonded onto the two major surfaces of the Ni-Mn-Ga plate using a conductive silver epoxy. The field was removed after the conductive silver epoxy was fully cured at room temperature to avoid the presence of austenitic phase in the plate. The electrodes of the two PVDF films were connected in such way that the two PVDF films were electrically in parallel.

The magnetomechanical testing of both the sandwich composite and monolithic crystal was performed using an automated setup built in-house [8]. A mechanical load (σ) was supplied by energizing a spring actuator toward the sample under test along the length (or [001]) direction. An electromagnet driven by a dynamic signal analyzer (CF5220, Ono Sokki, Yokohama, Japan) via a current-supply amplifier (TEC7572, AE Techron Inc., Elkhart, IN) was used to provide a sinusoidal magnetic field (H) of 10 kOe (peak) at a frequency of 0.1 Hz in the thickness (or [100]) direction. A Hall probe situated adjacent to the sample and connected to a Gaussmeter (7030, F. W. Bell, Orlando, FL) was employed to monitor H. The MFIS from the sample was measured by a laser displacement sensor (LK-G82, Keyence, Osaka, Japan) connected to a controller (LK-G3001, Keyence) with a resolution of 0.1 μm. All data were collected by the dynamic signal analyzer under the control of a computer. It should be noted that each sample was subject to a mechanical preload of 3.5 MPa along the length (or [001]) direction for a period of 3 min before a magnetomechanical test. This preloading process has shown to effectively reset any multivariant states to an initial nearly single-variant state in the sample [8], thus allowing for a direct comparison of all mechanical loading conditions to be discussed in Section III.

The ME coefficient (α_E) of the sandwich composite, defined as an induced electric field strength from the PVDF films in response to an applied ac magnetic field strength to the Ni-Mn-Ga plate ($\alpha_E = dE_3/dH_3$), was characterized by applying an ac magnetic drive field (H_3) up to 5 Oe (peak) at a frequency of 1 kHz superimposed on a dc magnetic bias field (H_{Bias}) up to 12 kOe (Fig. 1). H_3 was provided by a pair of Helmholtz coils driven by the dynamic signal analyzer via the current-supply amplifier. H_{Bias} was generated by the electromagnet with a dc power supply (DHP20015, Sorensen, San Diego, CA). Two Hall probes situated adjacent to the sample under test and connected to the Gaussmeter were employed to monitor H_3 and H_{Bias}. E_3 was acquired by measuring the electric charge (Q_3) generated from the electrodes (with parallel connection) of the PVDF films using a charge meter (5015, Kistler, Amherst, NY) and then by calculation using the relation: $E_3 = Q_3/(C_p\, t_p)$, where C_p is the capacitance of the PVDF films as determined by an impedance analyzer (4294, Agilent Technologies, Santa Clara, CA) at 1 kHz and t_p is the thickness of the PVDF films (0.11 mm in our case).

III. RESULTS AND DISCUSSION

Fig. 1 shows the configuration and working principle of the PVDF/Ni-Mn-Ga/PVDF sandwich composite in the absence [Fig. 1(a)] and presence [Fig. 1(b)] of a dc magnetic bias field (H_{Bias}). The composite is placed in the Cartesian coordinate system such that its length is along the 1-direction, and its thickness is in the 3-direction. In Fig. 1(a), the lightest block, with a horizontal arrow, de-

notes the Ni-Mn-Ga plate with an initial nearly single-variant state, whereas the darkest blocks represent the PVDF films, having a thickness polarization. It is recalled that the MFIS effect in the sandwich composite originates from a reorientation of martensitic twin variants under an applied magnetic field as a result of magnetocrystalline anisotropy in the Ni-Mn-Ga plate [1]–[3]. In the presence of an H_{Bias} along the thickness (or 3-) direction of the sandwich composite, a new twin variant, indicated by the slightly darker areas with downward-pointing arrows in Fig. 1(b), will occur at the expense of the preset initial nearly single-variant state of the Ni-Mn-Ga plate. This causes the Ni-Mn-Ga plate to produce a dc mechanical strain ($S_{1,m,dc}$) along the length (or 1-) direction. The subsequent introduction of an ac magnetic drive field (H_3) leads to an ac mechanical strain ($S_{1,m}$) superimposing on $S_{1,m,dc}$. The dc- and ac-MFIS effects in both the monolithic crystal and sandwich composite are reported in this section, together with the ME effect in the sandwich composite, at different mechanical loads (σ).

A. Magnetic Field-Induced Strain (MFIS) Effect

Fig. 2 shows the MFISs of the monolithic crystal [Fig. 2(a)] and sandwich composite [Fig. 2(b)] under different mechanical loads (σ) for the first one and one-quarter cycles of the applied magnetic field (H). Fig. 2(a) also includes various illustrations to depict the evolution of twin variants at load-free ($\sigma = 0$ MPa) condition for the monolithic crystal. Referring to the load-free case for the monolithic crystal in Fig. 2(a), the lighter region with a horizontal arrow in illustration O represents the initial nearly single-variant state (state I). By positively increasing H to about 4.5 kOe, there is no obvious increase in MFIS because of the pinning of twin boundary [7]. Once H is increased beyond this critical value, an easy reversible reorientation of twin variants is initiated and a new variant state appears and grows rapidly at the expense of the other as indicated by the darker region with an upward-pointing arrow in illustration A, resulting in a rapid increase in MFIS. Further increasing H to 9.5 kOe causes the new variant state to grow to a new nearly single-variant state (state II) as in illustration B, leading to a saturation MFIS of 5.6%. When H is reduced back to zero (at remanence), state II is almost preserved by the irreversible reorientation of twin variants as shown in illustration C, giving a gradual decrease in MFIS with a remanent strain of 5.3%. By applying a negative H, there is a 180° rotation in magnetization vectors associated with the two variant states in illustration D compared with illustration C. Further increasing the negative H to saturation at -9.5 kOe makes the variant state having the darker regions with downward-pointing arrows in illustration D to grow to a nearly single-variant state similar to state II but with an opposite magnetization vector as shown in illustration E. A subsequent cycling H recovers the MFIS curve depicted by illustrations C, B, C, E, etc. For the loaded cases in Fig. 2(a), although the MFIS curves exhibit a strong de-
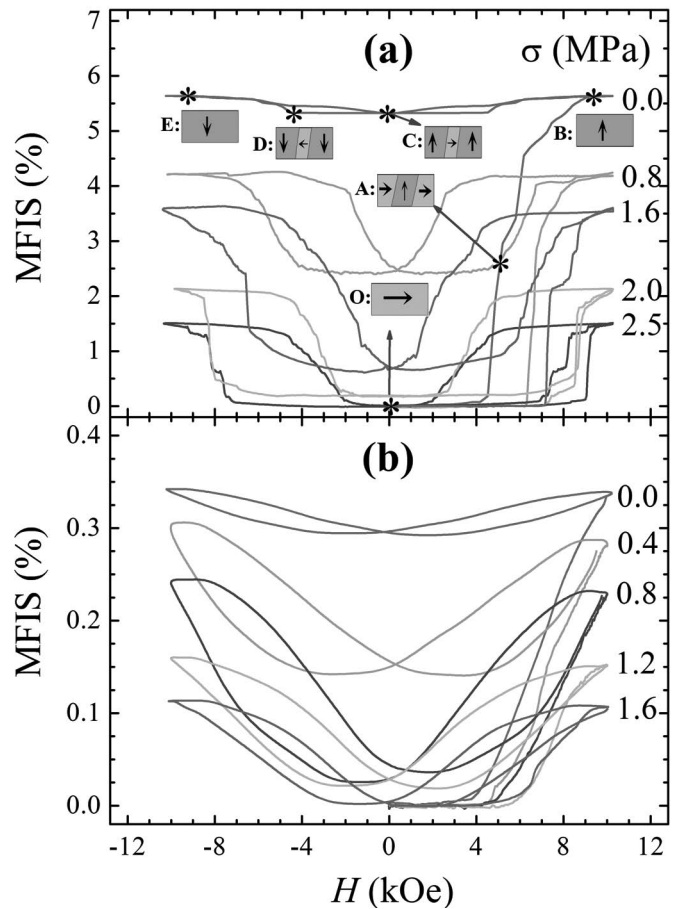

Fig. 2. MFISs of (a) monolithic Ni-Mn-Ga crystal and (b) PVDF/Ni-Mn-Ga/PVDF sandwich composite under different mechanical loads (σ) for the first one and one-quarter cycles of the applied magnetic field (H). Various illustrations depicting the evolution of twin variants at load-free condition are also included in (a) for the monolithic crystal.

pendence on σ, they have similar quantitative trends to the load-free case. However, a distinct difference is observed for the ones with $\sigma \geq 2.5$ MPa, in that the MFIS curves are fully reversible without remanent strains. For the sandwich composite in Fig. 2(b), the MFIS curves, in general, decline dramatically from those of the monolithic crystal in Fig. 2(a). That is, the load-free MFIS is saturated at a much lower level of 0.35% in the sandwich composite rather than at a high level of 5.6% in the monolithic crystal. The observation can be explained by the clamping of twin-boundary motion in the Ni-Mn-Ga plate by the PVDF films in the sandwich composite and means that a smaller volume fraction of state II in the Ni-Mn-Ga plate is involved in the reorientation of twin variants. Also, the loaded MFIS curves demonstrate a great dependence on σ and become fully reversible at a much reduced σ of 1.6 MPa.

To better understand the effect of σ on MFIS, we regard the first quarter-cycle and subsequent one cycle of MFIS curves in Fig. 2 as the dc- and ac-MFISs, respectively, and plot the dependences of dc-MFIS, remanent strain, and ac-MFIS on σ in Fig. 3 for the monolithic crystal [Fig. 3(a)] and the sandwich composite [Fig. 3(b)]. Here, the
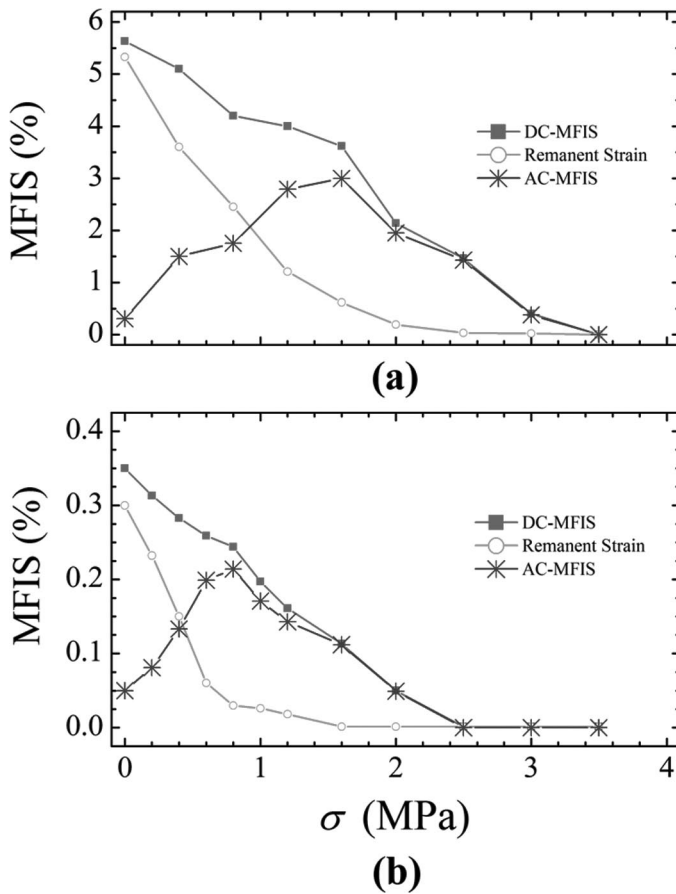
Fig. 3. Dependences of dc-MFIS, remanent strain, and ac-MFIS on applied mechanical load (σ) for (a) monolithic Ni-Mn-Ga crystal and (b) PVDF/Ni-Mn-Ga/PVDF sandwich composite.

reported dc-MFIS, remanent strain, and ac-MFIS values are the MFIS values at saturation, at remanence, and between saturation and remanence, respectively. From Fig. 3, the monotonic decrease in dc-MFIS for both the monolithic crystal and sandwich composite with the increase in σ reflects the use of magnetic field energy to overcome the increased mechanical load energy rather than to facilitate a reorientation of twin variants. As σ is elevated to a certain level, the reorientation of twin variants is completely inhibited. That is, the dc-MFIS is completely blocked at 3.5 and 2.5 MPa for the monolithic crystal and the sandwich composite, respectively. This means that a 3.5 MPa preload is large enough to block our samples and to reset any multivariant states to an initial nearly single-variant state. [e.g., illustration O in Fig. 2(a)]. This is further evident by the excellent agreement between the theoretical maximum lattice strain of 5.7%, the measured load-free dc-MFIS of 5.6%, and the manufacturer's load-free dc-MFIS of 5.6% in the monolithic crystal. Therefore, this 3.5 MPa preload was used to reset all our samples before a magnetomechanical test in Section II. Similar to dc-MFIS, the remanent strain decreases with the increase in σ and becomes zero at 2.5 and 1.8 MPa for the monolithic crystal and the sandwich composite, respectively. However, the ac-MFIS for both samples first increases and

then deceases. The optimal ac-MFIS is 3% at 1.6 MPa for the monolithic crystal and 0.22% at 0.8 MPa for the sandwich composite. The reason for the decrease in the optimal σ in the sandwich composite can be explained by the additional elastic load provided by the elastic shrinkage stress induced in the PVDF films.

B. Magnetoelectric (ME) Effect

Although the dc- and ac-MFISs in the sandwich composite are much smaller than those in the monolithic crystal (Figs. 2 and 3), they are still larger than the magnetostrictive strain ($\sim$0.16%) of the leading magnetostrictive alloy Tefernol-D. It is thus believed that a giant ME effect can be realized in our sandwich composite.

The mechanism of the ME effect in the sandwich composite is essentially based on the product property of the MFIS effect in the Ni-Mn-Ga plate and the piezoelectric effect in the PVDF films, which are mediated by mechanical stress. The working principle of the sandwich composite is as follows (Fig. 1): a dc magnetic bias field (H_{Bias}) applied along the thickness (or 3-) direction of the sandwich composite alters the preset initial nearly single-variant state of the Ni-Mn-Ga plate by introducing a new twin variant into the plate. This causes the Ni-Mn-Ga plate to produce a dc mechanical strain ($S_{1,\mathrm{m,dc}}$) along the length (or 1-) direction. The subsequent introduction of an ac magnetic drive field (H_3) leads to an ac mechanical strain ($S_{1,\mathrm{m}}$) superimposing on $S_{1,\mathrm{m,dc}}$. These strains ($S_{1,\mathrm{m}}$ and $S_{1,\mathrm{m,dc}}$) will be transferred to the PVDF films through mechanical coupling and will stress the PVDF films to generate an electric voltage (V_3) across the thickness (t_{p}) of the PVDF films because of the piezoelectric effect. Thus, the ME effect in the sandwich composite involves the conversion from H_3 to V_3 by mechanical mediation at given H_{Bias} and δ.

Fig. 4 plots the ac mechanical strain ($S_{1,\mathrm{m}}$) as a function of applied ac magnetic drive field (H_3) for the sandwich composite at a frequency of 1 kHz under various dc magnetic bias field (H_{Bias}) in load-free [Fig. 4(a)] and 0.8 MPa load [Fig. 4(b)] conditions. The insets show the dependences of piezomagnetic coefficient ($d_{31,\mathrm{m}}$) on H_{Bias}. The values of $d_{31,\mathrm{m}}$ are determined from the slopes of the $S_{1,\mathrm{m}}$–H_3 curves. It is clear that $S_{1,\mathrm{m}}$ has good linear responses to H_3 under various H_{Bias} in both load-free and 0.8 MPa load conditions. $d_{31,\mathrm{m}}$ shows strong dependences on H_{Bias} with the largest $d_{31,\mathrm{m}}$ found to be 2.6 nm/A at H_{Bias} = 8.35 kOe in load-free condition and 1.7 nm/A at H_{Bias} = 10.7 kOe in 0.8 MPa load condition. In fact, the $d_{31,\mathrm{m}}$–H_{Bias} curves in the sandwich composite originate from the easy reversible reorientation of twin variants as described by the MFIS curves in Fig. 2(b) [27].

Fig. 5 shows the induced electric voltage (V_3) as a function of applied ac magnetic drive field (H_3) for the sandwich composite at a frequency of 1 kHz under various dc magnetic bias fields (H_{Bias}) in load-free [Fig. 5(a)] and 0.8 MPa load [Fig. 5(b)] conditions. It is seen that V_3 exhibits good linearity with H_3 for different H_{Bias}. The
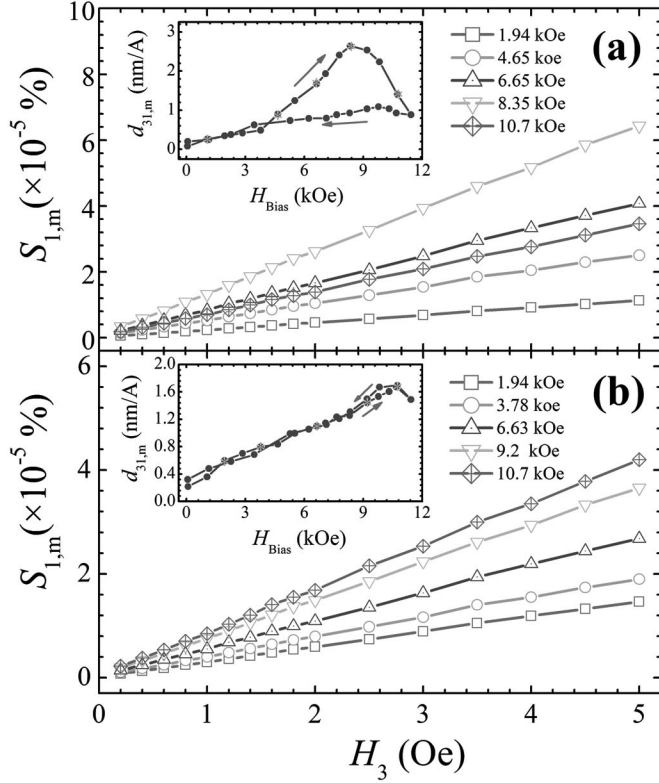
Fig. 4. AC mechanical strain ($S_{1,m}$) as a function of applied ac magnetic drive field (H_3) for PVDF/Ni-Mn-Ga/PVDF sandwich composite at a frequency of 1 kHz under various dc magnetic bias fields (H_{Bias}) in (a) load-free and (b) 0.8 MPa load conditions. The insets show the dependences of piezomagnetic coefficient ($d_{31,m}$) on H_{Bias}.

Fig. 5. Induced electric voltage (V_3) as a function of applied ac magnetic drive field (H_3) for PVDF/Ni-Mn-Ga/PVDF sandwich composite at a frequency of 1 kHz under various dc magnetic bias fields (H_{Bias}) in (a) load-free and (b) 0.8 MPa load conditions. The inset in (a) shows the waveforms of V_3 and H_3 (3.5 Oe) at $H_{Bias} = 8.35$ kOe.

largest ME coefficient (α_E), which is the largest slope of the V_3–H_3 curve divided by t_p (0.11 mm), is found to be 0.58 V/cm·Oe at $H_{Bias} = 8.35$ kOe for load-free condition and 0.42 V/cm·Oe at $H_{Bias} = 10.7$ kOe for 0.8 MPa load condition. The inset of Fig. 5(a) shows the waveforms of V_3 and H_3 (3.5 Oe) at $H_{Bias} = 8.35$ kOe. V_3 and H_3 are of opposite phase. V_3 follows H_3 steadily, reflecting the ability of stable signal conversion from H_3 to V_3 in our composite.

Because of the existence of generally large hysteresis effect in Ni-Mn-Ga crystals, the dynamic behavior of the crystals can be described by pseudo-piezomagnetism. The pseudo-piezomagnetic coefficient ($d_{31,m}$) at given H_{Bias} and δ can be assumed to be constant [27]. In this way, the pseudo-piezomagnetism in the Ni-Mn-Ga plate of the sandwich composite at given H_{Bias} and δ can be expressed by the constitutive piezomagnetic equations as follows [12]:

$$S_{1,m} = s_{11,m}^H \cdot T_{1,m} + d_{31,m} \cdot H_3$$
$$B_1 = d_{31,m} \cdot T_{1,m} + \mu_{31}^T \cdot H_3, \tag{1}$$

where H_3 and B_1 are the magnetic field strength along the thickness direction and the magnetic induction along the length direction, respectively; $T_{1,m}$ and $S_{1,m}$ are the mechanical stress and strain along the length direction, respectively; $d_{31,m}$ is the pseudo-piezomagnetic coefficient;
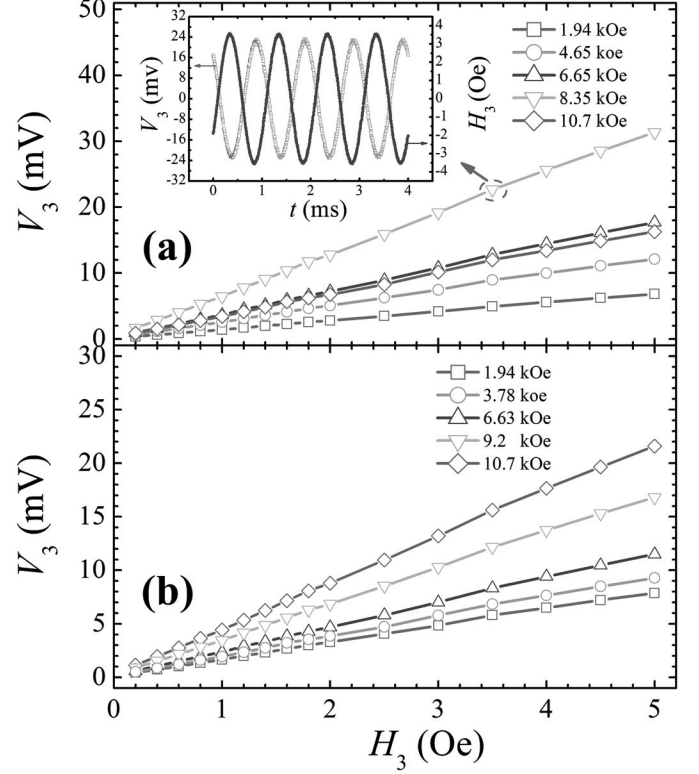
$s_{11,m}^H$ is the elastic compliance coefficient at constant magnetic field strength; and μ_{31}^T is the magnetic permeability at constant stress. For the PVDF films, the constitutive piezoelectric equations are adopted as follows [28], [29]:

$$S_{1,p} = s_{11,p}^D \cdot T_{1,p} + g_{31,p} \cdot D_3$$
$$E_3 = -g_{31,p} \cdot T_{1,p} + \frac{1}{\varepsilon_{33}^T} \cdot D_3, \tag{2}$$

where E_3 and D_3 are the electric field strength and electric displacement along the thickness direction, respectively; $T_{1,p}$ and $S_{1,p}$ are the mechanical stress and strain along the length direction, respectively; $g_{31,p}$ is the piezoelectric voltage coefficient; $s_{11,p}^D$ is the elastic compliance coefficient at constant electric displacement, and ε_{33}^T is the dielectric permittivity at constant stress. The boundary conditions for the sandwich composite are

$$T_{1,m} \cdot t_m = -T_{1,p} \cdot t_p$$
$$S_{1,m} = S_{1,p}, \tag{3}$$

where t_m and t_p are the thickness of the Ni-Mn-Ga plate and that of the PVDF films, respectively. Combining (1), (2), and (3), and setting $D_3 = 0$ in (2), the ME coefficient (α_E) of the sandwich composite is
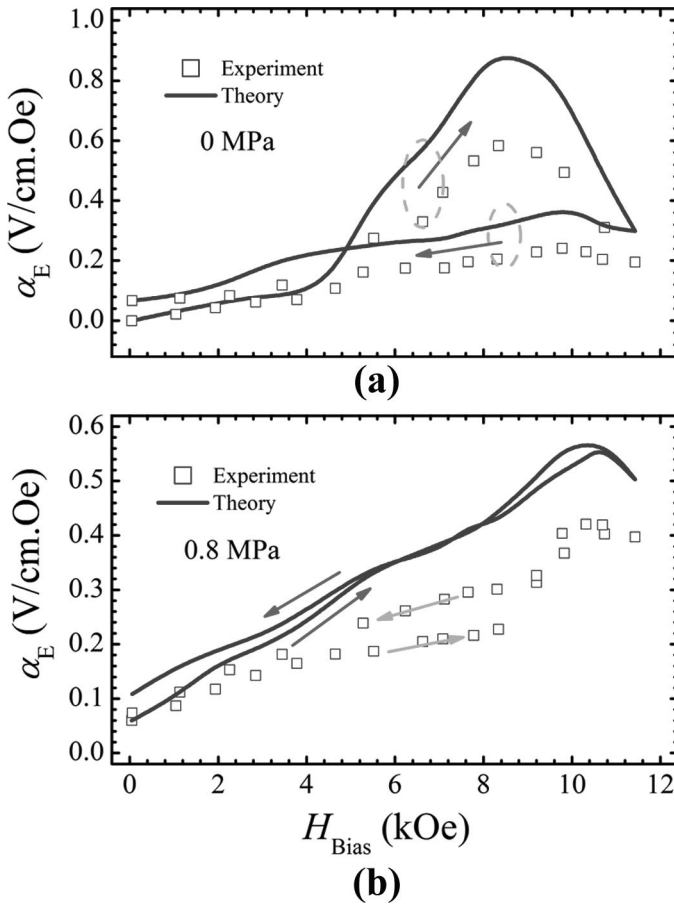
Fig. 6. Comparison between the experimental (symbols) and theoretical (lines) α_E as a function of dc magnetic bias field (H_{Bias}) for the sandwich composite in (a) load-free and (b) 0.8 MPa load conditions.

$$\alpha_{\text{E}} = dE_3/dH_3 = -\frac{d_{31,\text{m}} \cdot g_{31,\text{p}} \cdot t_{\text{m}}}{s_{11,\text{m}}^H \cdot t_{\text{p}} + s_{11,\text{p}}^D \cdot t_{\text{m}}}. \qquad (4)$$

From (4), it is clear that α_{E} of the sandwich composite depends on $d_{31,\text{m}}$, $s_{11,\text{m}}^H$, and t_{m} of the Ni-Mn-Ga plate as well as $g_{31,\text{p}}$, $s_{11,\text{p}}^D$, and t_{p} of the PVDF films. It is noted that $d_{31,\text{m}}$ and $g_{31,\text{p}}$ are positive, and the minus sign associated with α_E indicates an opposite phase relationship between E_3 and H_3. This is consistent with the experimental result shown in the inset of Fig. 5(a).

Fig. 6 displays the comparison between the experimental (symbols) and theoretical (lines) α_E as a function of H_{Bias} for the sandwich composite in load-free [Fig. 6(a)] and 0.8 MPa load [Fig. 6(b)] conditions. The experimental α_E values are those obtained from the slopes of the V_3–H_3 plots divided by t_{p} (0.11 mm) at different H_{Bias} in Fig. 5. The theoretical α_E values are those calculated by (4) based on the measured $d_{31,\text{m}}$–H_{Bias} plots in the insets of Fig. 4. It is obvious that the experimental and theoretical α_E are in good agreement. Besides, it is noted that the variation of α_E with H_{Bias} in Fig. 6 is very similar to that of $d_{31,\text{m}}$ with H_{Bias} in the insets of Fig 4. This suggests that the MFIS effect in the Ni-Mn-Ga plate controls predominantly the ME effect in the sandwich composite.

Particularly, the reversible reorientation of twin variants in the Ni-Mn-Ga plate under a small H_3 superimposed on an optimal H_{Bias} (8.35 kOe under load-free condition) is the main reason for the largest α_E (0.58 V/cm·Oe) in our composite. However, it is required to sustain the reversible reorientation of twin variants in the Ni-Mn-Ga plate by an external stress loading [1]–[8], [27]. In our composite, it is the stress induced in the PVDF films during actuation of the Ni-Mn-Ga plate, giving a recoverable stress for the Ni-Mn-Ga plate.

IV. CONCLUSION

A sandwich composite consisting of one FSM Ni-Mn-Ga crystal plate and two piezoelectric PVDF polymer films has been fabricated. The MFIS effect in the sandwich composite has been studied, together with a monolithic crystal, at various mechanical loads. The ME effect in the sandwich composite has also been studied, both experimentally and theoretically, with good agreement. Smaller MFISs have been found in the composite than the monolithic crystal because of the clamping of martensitic twin-boundary motion in the Ni-Mn-Ga plate by the PVDF films. The mechanism of the ME effect has been attributed to the mechanically mediated MFIS effect in the Ni-Mn-Ga plate and piezoelectric effect in the PVDF films. The largest α_E of 0.58 V/cm·Oe obtained at an optimal H_{Bias} of 8.35 kOe under load-free condition has been found to result from the reversible reorientation of martensitic twin variants in the Ni-Mn-Ga plate.

REFERENCES

[1] K. Ullakko, J. K. Huang, C. Kantner, R. C. O'Handley, and V. V. Kokorin, "Large magnetic-field-induced strains in Ni$_2$MnGa single crystals," *Appl. Phys. Lett.*, vol. 69, pp. 1966–1968, Sep. 1996.

[2] H. D. Chopra, C. Ji, and V. V. Kokorin, "Magnetic-field-induced twin boundary motion in magnetic shape-memory alloys," *Phys. Rev. B*, vol. 61, pp. R14913–R14915, Jun. 2000.

[3] S. J. Murray, M. Marioni, S. M. Allen, R. C. O'Handley, and T. A. Lograsso, "6% magnetic-field-induced strain by twin-boundary motion in ferromagnetic Ni-Mn-Ga," *Appl. Phys. Lett.*, vol. 77, pp. 886–888, Aug. 2000.

[4] A. Sozinov, A. A. Likhachev, N. Lanska, and K. Ullakko, "Giant magnetic field-induced strain in NiMnGa seven-layered martensitic phase," *Appl. Phys. Lett.*, vol. 80, pp. 1746–1748, Mar. 2002.

[5] A. Sozinov, A. A. Likhachev, and K. Ullakko, "Crystal structures ad magnetic anisotropy properties of Ni-Mn-Ga martensitic phases with giant magnetic field-induced strain," *IEEE Trans. Magn.*, vol. 38, pp. 2814–2816, Sep. 2002.

[6] C. P. Henry, D. Bono, J. Feuchtwanger, S. M. Allen, and R. C. O'Handley, "AC field-induced actuation of single crystal Ni-Mn-Ga," *J. Appl. Phys.*, vol. 91, pp. 7810–7811, May 2002.

[7] H. E. Karaca, I. Karaman, B. Basaran, Y. I. Chumlyakov, and H. J. Maier, "Magnetic field and stress induced martensite reorientation in NiMnGa ferromagnetic shape memory alloy single crystals," *Acta Mater.*, vol. 54, pp. 233–245, Oct. 2006.

[8] M. Zeng, S. W. Or, and H. L. W. Chan, "DC- and ac-magnetic field induced strain effects in ferromagnetic shape memory composites of Ni–Mn–Ga single crystal and polyurethane polymer," *J. Appl. Phys.*, vol. 107, art. no. 09A942, May 2010.

[9] S. W. Or, N. Nersessian, and G. P. Carman, "Dynamic magnetomechanical behavior of Terfenol-D/epoxy 1-3 particulate composites," *IEEE Trans. Magn.*, vol. 40, pp. 71–74, Jan. 2004.

[10] S. W. Or, N. Nersessian, G. P. McKnight, and G. P. Carman, "Dynamic magnetomechanical properties of [112]-oriented Terfenol-D/epoxy 1–3 magnetostrictive particulate composites," *J. Appl. Phys.*, vol. 93, pp. 8510–8512, May 2003.

[11] S. W. Or, T. L. Li, and H. L. W. Chan, "Dynamic magnetomechanical properties of Terfenol-D/epoxy pseudo 1–3 composites," *J. Appl. Phys.*, vol. 97, art. no. 10M308, May 2005.

[12] G. Engdahl, *Magnetostrictive Materials Handbook*, New York, NY: Academic, 2000.

[13] L. D. Landau and E. Lifshitz, *Electrodynamics of Continuous Media*, Oxford, UK: Pergamon, 1960.

[14] M. Fiebig, "Revival of the magnetoelectric effect," *J. Phys. D*, vol. 38, pp. R123–R152, Apr. 2005.

[15] V. J. Folen, G. T. Rado, and E. W. Stalder, "Anisotropy of the magnetoelectric effect in Cr_2O_3," *Phys. Rev. Lett.*, vol. 6, pp. 607–608, Jun. 1961.

[16] G. L. Yuan, K. Z. Baba-Kishi, J.-M. Liu, S. W. Or, Y. P. Wang, and Z. G. Liu, "Multiferroic properties of single-phase $Bi_{0.85}La_{0.15}FeO_3$ lead-free ceramics," *J. Am. Ceram. Soc.*, vol. 89, pp. 3136–3139, Oct. 2006.

[17] G. L. Yuan, S. W. Or, and H. L. W. Chan, "Structural transformation and ferroelectric-paraelectric phase transition in $Bi_{1-x}La_xFeO_3$ (x=0–0.25) multiferroic ceramics," *J. Phys. D*, vol. 40, pp. 1196–1200, Feb. 2007.

[18] M. Zeng, J. G. Wan, Y. Wang, H. Yu, J.-M. Liu, X. P. Jiang, and C. W. Nan, "Resonance magnetoelectric effect in bulk composites of lead zirconate titanate and nickel ferrite," *J. Appl. Phys.*, vol. 95, pp. 8069–8073, Jun. 2004.

[19] H. F. Zhang, S. W. Or, and H. L. W. Chan, "Multiferroic properties of $Ni_{0.5}Zn_{0.5}Fe_2O_4$–$Pb(Zr_{0.53}Ti_{0.47})O_3$ ceramic composites," *J. Appl. Phys.*, vol. 104, art. no. 104109, Nov. 2008.

[20] S. G. Lu, Z. K. Xu, Y. P. Wang, S. S. Guo, T. L. Haydn, C. Li, and S. W. Or, "Effect of $CoFe_2O_4$ content on the dielectric and magnetoelectric properties in $Pb(ZrTi)O_3/CoFe_2O_4$ composite," *J. Electroceram.*, vol. 21, pp. 398–400, Sep. 2008.

[21] J. X. Zhang, J. Y. Dai, L. C. So, C. L. Sun, C. Y. Lo, S. W. Or, and H. L. W. Chan, "The effect of magnetic nanoparticles on the morphology, ferroelectric, and magnetoelectric behaviors of CFO/P(VDF-TrFE) 0–3 nanocomposites," *J. Appl. Phys.*, vol. 105, art. no. 054102, Mar. 2009.

[22] J. Ryu, C. A. Vásquez, K. Uchino, and H. E. Kim, "Magnetoelectric properties in piezoelectric and magnetostrictive laminate composites," *Jpn. J. Appl. Phys.*, vol. 40, pp. 4948–4951, Aug. 2001.

[23] S. X. Dong, J. F. Li, and D. Viehland, "A longitudinal-longitudinal mode Terfenol-D/$Pb(Mg_{1/3}Nb_{2/3})O_3$–$PbTiO_3$ laminate composite," *Appl. Phys. Lett.*, vol. 85, pp. 5305–5307, Nov. 2004.

[24] S. S. Guo, S. G. Lu, Z. Xu, X. Z. Zhao, and S. W. Or, "Enhanced magnetoelectric effect in Terfenol-D and flextensional cymbal laminates," *Appl. Phys. Lett.*, vol. 88, art. no. 182906, May 2006.

[25] Y. M. Jia, S. W. Or, J. Wang, H. L. W. Chan, X. Y. Zhao, and H. S. Luo, "High magnetoelectric effect in laminated composites of giant magnetostrictive alloy and lead-free piezoelectric ceramic," *J. Appl. Phys.*, vol. 101, art. no. 104103, May 2007.

[26] Y. J. Wang, S. W. Or, H. L. W. Chan, X. Y. Zhao, and H. S. Luo, "Enhanced magnetoelectric effect in longitudinal-transverse mode Terfenol-D/$Pb(Mg_{1/3}Nb_{2/3})O_3$–$PbTiO_3$ laminate composites with optimal crystal cut," *J. Appl. Phys.*, vol. 103, art. no. 124511, Jun. 2008.

[27] M. Zeng, S. W. Or, and H. L. W. Chan, "Large magnetoelectric effect from mechanically mediated magnetic field-induced strain effect in Ni–Mn–Ga single crystal and piezoelectric effect in PVDF polymer," *J. Alloy. Comp.*, vol. 490, pp. L5–L8, Oct. 2010.

[28] *IEEE Standard on Piezoelectricity*, ANSI/IEEE Standard 176–1987, 1987.

[29] S. W. Or and H. L. W. Chan, "Mode coupling in lead zirconate titanate/epoxy 1–3 piezocomposite rings," *J. Appl. Phys.*, vol. 90, pp. 4122–4129, Oct. 2001.

Min Zeng received the B.Sc. and M.Sc. degrees in materials science and engineering from the Jingdezhen Ceramic Institute, China, in 1999 and 2004, respectively.

He is currently a Ph.D. student in the Department of Electrical Engineering and the Department of Applied Physics at The Hong Kong Polytechnic University, working on ferromagnetic shape memory alloys and their composites.

Siu Wing Or received the B.Sc.(1st Class Honors), M.Phil., and Ph.D. degrees in engineering physics from The Hong Kong Polytechnic University (PolyU) in 1995, 1997, and 2001, respectively.

He was a teaching company associate, a R&D electronic engineer, and a senior R&D electronic engineer in ASM Assembly Automation Ltd., Hong Kong, from 1995 to 2001. He then worked as a postdoctoral research fellow in the Mechanical and Aerospace Engineering Department at the University of California, Los Angeles, CA, for 1.5 years before he joined PolyU as a lecturer in materials science and technology in the Department of Applied Physics in 2002.

Dr. Or is currently an associate professor in utilization and the director of Multifunctional Materials and Systems Laboratory in the Department of Electrical Engineering at PolyU. He is a senior member of IEEE and a member of ASME.

Helen Lai Wa Chan received the B.Sc. and M. Phil. degrees in physics from the Chinese University of Hong Kong in 1970 and 1974, respectively, and the Ph.D. degree in physics from Macquarie University, Australia, in 1987.

She worked as a research scientist in the National Measurement Laboratory of the CSIRO Division of Applied Physics, Sydney, Australia from 1987 to 1991, where she was responsible for setting up the Australian Standards for medical ultrasound transducer calibration. She then worked as a senior acoustic engineer at GEC-Marconi Pty., Australia, for a year on hydrophone arrays for underwater acoustics before she returned to Hong Kong in 1992.

Prof. Chan is currently the chair professor and head of applied physics at The Hong Kong Polytechnic University. She is a senior member of IEEE.